Washington University School of Medicine
Digital Commons@Becker

Open Access Publications

7-1-2013

Counting unstained, confluent cells by modified bright-field microscopy

L. Louis Drey

Michael Graber

Jan Bieschke

Follow this and additional works at: https://digitalcommons.wustl.edu/open_access_pubs

Reports

Reports

Counting unstained, confluent cells by modified bright-field microscopy

L. Louis Drey†, Michael C. Graber, and Jan Bieschke
Washington University in St. Louis, Department of Biomedical Engineering, St. Louis, MO

†L.L.D.'s current address is St. Louis, MO, USA.

BioTechniques 55:28-33 (July 2013) doi 10.2144/000114056
Keywords: brightfield; microscopy; fluorescence; cell culture; cell counting; pinhole; monochromatic; PBS; defocusing

We present a very simple procedure yielding high-contrast images of adherent, confluent cells such as human neuroblastoma (SH-EP) cells by ordinary bright-field microscopy. Cells are illuminated through a color filter and a pinhole aperture placed between the condenser and the cell culture surface. Refraction by each cell body generates a sharp, bright spot when the image is defocused. The technique allows robust, automatic cell counting from a single bright-field image in a wide range of focal positions using free, readily available image-analysis tools. Contrast may be enhanced by swelling cell bodies with a brief incubation in PBS. The procedure was benchmarked against manual and automated counting of fluorescently labeled cell nuclei. Counts from day-old and freshly seeded plates were compared in a range of densities, from sparse to densely overgrown. On average, bright-field images produced the same counts as fluorescence images, with less than 5% error. This method will allow routine cell counting using a plain bright-field microscope without cell-line modification or cell staining.

In cell culture experiments where the effect of one or more chemicals on cell number must be assessed, it would be ideal to know precisely how many cells have been plated into a well or a subregion of a well at the beginning of an experiment, how many cells were alive days later before addition of the chemical, and how many cells were present at the end of the experiment. This is especially true when subject chemicals affect cell proliferation, yet the experiment aims to quantitate a different parameter such as metabolic activity, which then needs to be normalized against cell number.

Counting cells is required when adherent mammalian cells are cultivated for numerous other experimental applications such as measuring protein overexpression or RNAi gene silencing. Each procedure may affect cellular growth, skewing measurement of the effects. When cells must be harvested and replated one or more times, traditional cell counting with a hemocytometer (1) can be time-consuming and error-prone.

Fluorescence microscopy is the most widely used method to visualize and quantitate cellular proteins. When cell proteins are quantitated, usually it is necessary to normalize the data as a ratio of cell number against total protein content. Cell counting from fluorescence images may readily be achieved (2). However, when common nuclear dyes such as Hoechst 33342 or DAPI are used, counts may be less than precise if the dyes themselves reduce cell viability or affect growth rates (2). Hence, such methods can impinge on data and thus skew results.

Alternately, cells may be engineered to express a nuclear protein, such as the histone protein H2B, that is fused to green fluorescent protein (GFP) in order to provide highly accurate cell counts (3). With this approach, creating new stable cell lines before every experiment may be required. Since GFP fluorescence microscopy uses one fluorescence channel, immunofluorescence analysis of other proteins may also be limited.

Such difficulties have prompted a search for alternative methods of cell counting using bright-field microscopy. Generally, bright-field microscopy of flat, adherent cells suffers because cultured cells are transparent. As a result, contrast is very poor, particularly when imaging is done in the growth plane itself. Several software-based algorithms have recently been developed to improve contrast in bright-field images (4–6). Counting cells is relatively easy for naturally round, individually growing cells such as yeast (7). However, when flat, adherent cells must be quantitated, digital holography (8), z-projection of multiple z-stacked images (9), or intensity derivation (10) may be required to improve contrast and allow cell counting. These methods require acquisition of multiple

REPRINT WITH PERMISSION ONLY

Method summary:

Unstained adherent cells are illuminated with monochromatic light through a pinhole aperture. In defocused bright-field images, each cell creates a bright spot that allows easy automated cell counting from single images. Contrast and counting accuracy can be further enhanced by brief swelling of cells in PBS.

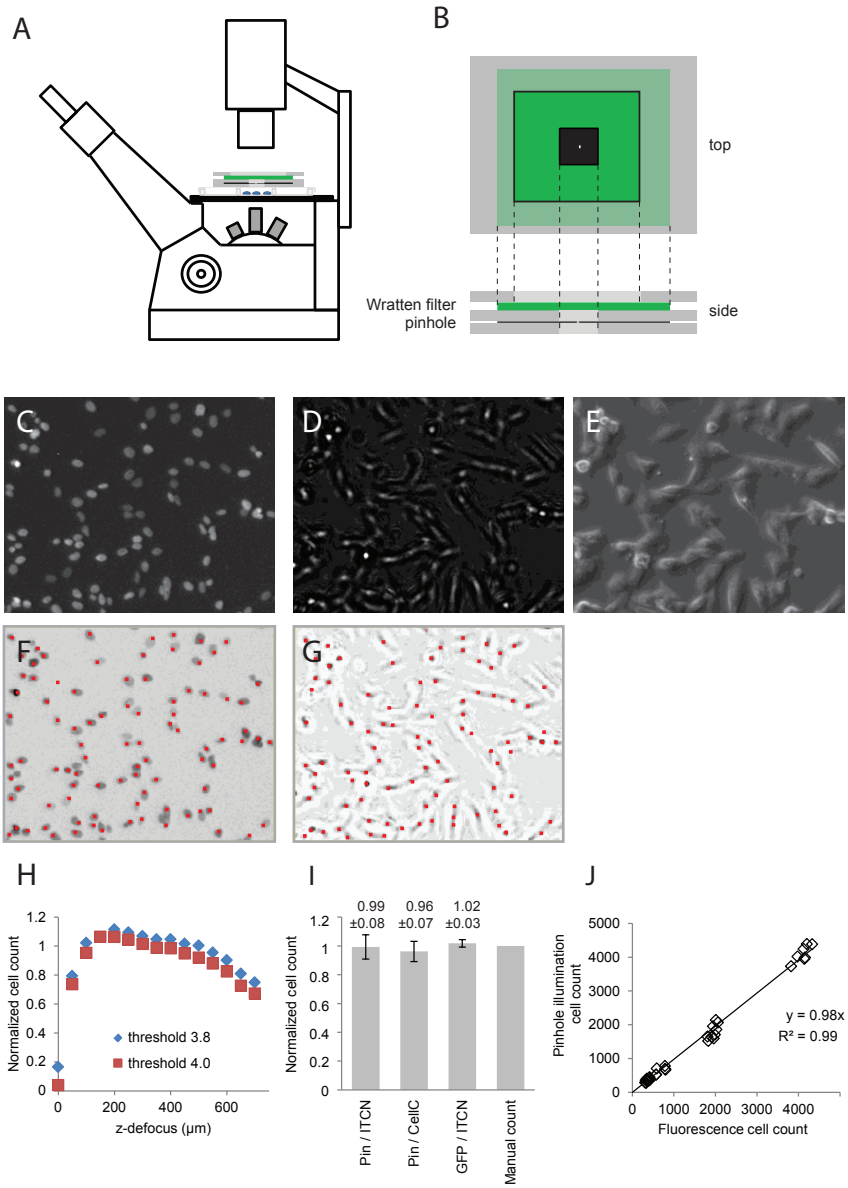

Figure 1. Cell counting from pinhole illuminated microscopy. (A) A pinhole aperture and a green Wratten filter were placed on top of the cell culture plate and positioned to ensure an even illumination of the viewing field. (B) Enlarged view of the filter-pinhole assembly. SHEP-GFP cells were seeded at 50,000–500,000 per well in a 12-well plate and grown for 2 days with a media switch after 24 h. Panels (C-G) show enlarged sections of images recorded in parallel at 4× magnification: (C) GFP fluorescence, (D) Pinhole illuminated bright-field image, (E) Phase contrast image, (F) Cell identification from fluorescence images, and (G) pinhole illuminated bright-field images calculated by the ImageJ ITCN plugin; red spots mark identified cells. Cell markers were enlarged 400% to improve readability. (H) Cell counts from pinhole images recorded at different focal positions normalized against counts from fluorescence images. (I) Comparison of cell counts from fluorescence and pinhole images analyzed by manual and automated counting (mean ± SD, n = 9). (J) Pinhole cell counts plotted against counts from GFP fluorescence fitted by linear regression.

images followed by application of an image analysis algorithm, making them best suited to automated, high content screening microscopy.

Here we present a simple procedure to generate high-contrast images of flat, adherent and possibly confluent cells. The resulting images can be analyzed with free, readily available software tools, such as the ITCN plugin for ImageJ (11) or CellC analysis software (12). Cells may be counted directly from single bright-field images. Our approach allows users to count cells using a standard microscope present in most cell culture laboratories. Furthermore, it does not necessitate tagging of cell lines with fluorescent dyes or any other method of nuclear staining.

Methods

Cell culture

Cell culture plates were pretreated with 0.1% poly-L-lysine solution for 15 min, washed 4 times, and stored at 4°C. Human neuroblastoma (SH-EP) cells expressing the GFP-tagged nuclear histone H2B protein (SHEP-GFP) were cultured in DMEM supplemented with 4.5 g/l D-glucose, 10% fetal bovine serum, 100 IU/mL penicillin, and 100 µg/mL streptomycin at 37°C/5% CO2. SHEP-GFP cells were plated at densities of 50,000–5 million per well in 12-well plates and grown overnight. Live cells were imaged directly in culture media. Alternatively, the culture media was suctioned and replaced by PBS for 15 min prior to imaging to induce swelling of cells.

Imaging

Images were acquired on an Olympus IX70 inverted fluorescence microscope (Olympus America Inc., Center Valley, NJ), using a 4×/0.13 NA Uplan air objective and a 2 megapixel Olympus MicroFire CCD camera. Parallel GFP fluorescence and pinhole illumination images were recorded for each growth region. Fluorescence images were recorded in-focus at exposure times of 300 ms, using the Fluorescein/GFP filter cube (U-MNIB). For pinhole illumination, cells were illuminated by the tungsten halogen lamp at full power with the condenser fully open, without phase rings or filters in the illumination path.

A green Kodak Wratten filter #58 (Edmund Optics, Barrington, NJ) and a 130 µm pinhole were affixed to a stabilizing cardboard frame. These were placed directly on the cell culture plate and positioned to achieve an even illumination of the viewing field (Figure 1 A, B).

The image was then defocused by lowering the objective until image contrast was maximal. Best results were achieved by lowering the focus by 50–200 µm, corresponding to 0.5–2 turns of the fine z-focus drive. An image was then taken using an 80 ms exposure. Exposure times for fluorescence and pinhole images were kept constant throughout the measurements.

The pinhole aperture was formed by punching a hole into heavy-duty (0.9 mil) aluminum foil with the point of a fine needle. The size of the pinhole was determined to be 130 ± 10 µm by placing the aperture on the bed of an optical scanner (MFC 7460, Brother, Bridgewater, NJ) and scanning the pinhole at 9600 dpi (n = 4).

Cell counting

Cells were counted using the ITCN (Image-based tool for counting nuclei) Plugin for ImageJ developed by Thomas Kuo and

Jiyun Byun at the Center for Bio-image Informatics at UC Santa Barbara (11). Its algorithm assumes nuclei to be blob-like structures with roughly convex local intensity distributions whose iso-level contour is approximately ellipsoidal; nuclei are fitted by an inverted Laplacian of Gaussian filter (11). The plugin can be downloaded without charge from www.bioimage.ucsb.edu/automatic-nuclei-counter-plug-in-for-imagej. Images were converted to eight-bit greyscale and inverted before using ITCN. Cell detection was performed by detecting dark peaks with the following parameters: cell width = 7, minimum distance = 7, threshold = 2, mask image: use selected ROI.

Alternatively, cells were counted using the CellC image analysis software (available for download at: https://sites.google.com/site/cellcsoftware/), which identifies cells by global thresholding combined with a watershed segmentation algorithm (12). Eight-bit images were loaded into the CellC software. The Automatic Intensity Threshold was adjusted to between 0.4 and 0.5. The number of cells was evaluated by counting the number of isolated pixel groups that exceeded the intensity threshold. As a reference, cells were also counted manually from brightfield images using the ImageJ cell counter plugin.

Image contrast and brightness have been optimized for publication in panels shown in Figures 1–3, but all cell counting data were calculated from unprocessed microscopy images.

Results and Discussion

Counting of neuroblastoma cells by pinhole illumination and fluorescence microscopy

Bright-field images, particularly those of adherent cells, lack contrast, which makes them ill-suited for automated cell counting algorithms. By placing a tiny pinhole aperture directly between the condenser lamp and experimental surface (Figure 1A, B) and by defocusing the image, bright-field images of very high contrast could be generated since each cell body produced a bright spot in a plane below the cells. We found that contrast could be further increased by placing a monochromatic filter in the beam path (Figure 1C). Image contrast was largely unchanged by altering the z-position of either the condenser or the pinhole assembly (data not shown).

SH-EP cells expressing GFP-tagged nuclear histone H2B (SHEP-GFP) were imaged using identical fields with pinhole illumination, GFP fluorescence, and conventional phase-contrast bright-field microscopy (Figure 1C, D, E). Three different regions in three independent wells were examined and cells were identified from fluorescence images and pinhole illuminated images using the ITCN plugin (Figure 1F, G).

We found that uniform ITCN variable settings (width, minimum distance, and threshold) could be used for all fluorescence images, while threshold values varying between 2 and 4 optimized imaging in the pinhole method. The latter effect resulted from slight differences in the overall brightness of images gathered from different microscope sessions. Width and minimum distance variables were kept constant for all pinhole images. We tested the influence of the z-focus position on counting accuracy by recording a stack of images while lowering the focal plane from -50µm to -700µm (Figure 1H). Cell counts were stable over a wide range of focus positions. While defocusing by ~50 µm produced the highest contrast, focal positions from -100 to -400 µm were more tolerant to variations in thickness of the cell culture plates and produced robust counting results (Figure 1H).

We compared counts obtained through several cell counting procedures. First, we automatically counted cells in identical pinhole illuminated images using ITCN and CellC cell counting software and compared those results with automated counts of fluorescence images. We also compared the results with manual cell counts (Figure 1I). Average counts for all methods diverged by less than 5%. Cells counted from fluorescence microscopy matched the manual count most closely (3% variation at 50,000 cells per well), whereas pinhole illumination resulted in a somewhat higher standard deviation (7%–8%). This is likely due to the presence of highly elongated cells that lowered contrast in pinhole images. In these images, diminished contrast sometimes prevented correct cell identification or led to double-counting of cells. Analysis of cells plated at a widely divergent densities (50,000–500,000 per well) confirmed that pinhole-based counts and counts generated from fluores-

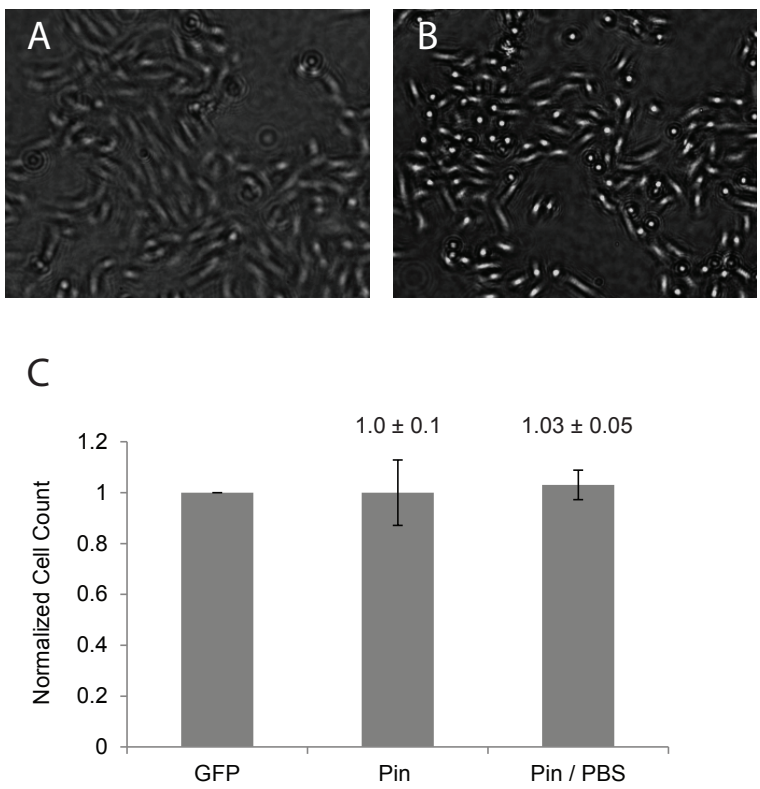

Figure 2. Cell counting after swelling by PBS treatment. SHEP-GFP cells were seeded at 1.5 million per well in a 12-well plate and grown for 2 days with media changed after 24 h. (A) Pinhole illuminated bright-field images were recorded in cell media. (B) In order to increase contrast in the images, complete media was exchanged for PBS. Cells were immersed in PBS for 15 min before imaging. Cells were counted as described in Figure 1. (C) Cell counts of pinhole illuminated images with and without PBS incubation were normalized against fluorescence images of the same viewing field (mean ± SD, n = 9).

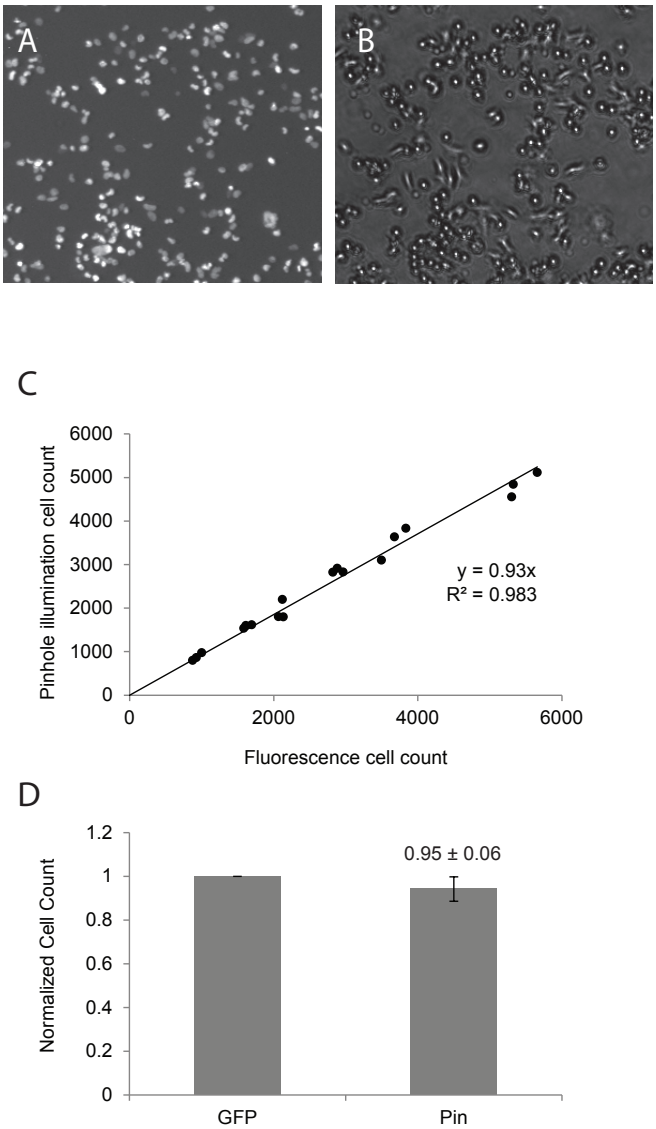

Figure 3. Counting of freshly seeded cells. SHEP-GFP cells were seeded at 100,000–1 million per well and were allowed to attach to the bottom of a 12-well plate for approximately 3 hours. (A) Fluorescence- and (B) pinhole-illuminated bright field images were taken in identical viewing fields of the freshly seeded cells. (C) Fluorescence and pinhole counts were plotted against one another and fitted by linear regression. (D) Normalized cell counts for corresponding fluorescence (GFP) and pinhole (Pin) images (mean ± SD, n = 18).

cence images were highly correlated ($R^2 > 0.98$) (Figure 1J); likewise these counts on average differed by less than 5%.

Brief cell swelling in PBS improves contrast and counting accuracy

We found that variability of cell counts from pinhole illumination images could be reduced by briefly removing growth media from the wells and replacing it with 1× PBS. Cells incubated in PBS for 15 min experienced overall swelling of the cell body, resulting in increased contrast during pinhole imaging (Figure 2A, B). After imaging, growth media was returned to the cell cultures. Re-counting cells after 24 h did not reveal any differences in cell number between PBS-treated and untreated cells; that is, the PBS treatment did not affect SH-EP cell viability. The increased contrast of PBS-treated cells resulted in substantially more accurate cell detection by the ITCN ImageJ plugin, decreasing the average standard deviation of cell counts from 10% in untreated cells to 5% after PBS treatment when benchmarked against fluorescence-based counting (Figure 2C).

Counting of freshly seeded cells

Often it is desirable to control for varied cell densities when cells are grown under different conditions (e.g., siRNA treatment) and re-seeded onto a new culture plate. When cells are round and have not fully spread out, they should be particularly good targets for pinhole illumination cell counting. To test the accuracy of the method under these conditions, we plated cells at different densities (50,000–500,000 per well). Freshly seeded cells were permitted to settle for three hours. Fluorescence and pinhole images from three independent wells were taken for each density (Figure 3A, B). Cells were imaged in their original growth media. Counts from fluorescence and pinhole images show a strong correlation ($R^2 > 0.98$) (Figure 3C). Cell counts from pinhole images are almost identical to those from nucleus fluorescence (95 ± 6%, Figure 3D). Cells were slightly undercounted in pinhole illuminated images at higher densities, likely due to clumping of cells under these conditions.

Counting of dense cell layers

To test the limitations of pinhole illumination counting of dense-to-overgrown cell layers, cells from the prior experiment were allowed to grow for an additional 24–48 h. This resulted in overgrown cell cultures where cells started to form a second overlapping layer. Overgrowth was a challenge for this method of automated cell counting since it was not possible to get all cells simultaneously into focus. Fluorescence and pinhole images were taken with and without treating the cells with PBS for 15 min. Cell counts were normalized against fluorescence imaging (Figure 4). Under these conditions, cell counts from pinhole images with and without PBS treatment were virtually identical to those obtained by fluorescence imaging, 101 ± 7% and 97 ± 2%, respectively. PBS treatment of cells substantially decreased the counting errors observed previously with lower cell densities.

Generally, brightfield microscopy can visualize differences in opacity (amplitude objects) while failing to resolve transparent objects that differ only in refractive index (phase objects), which are better viewed using phase contrast microscopy (13). However, phase objects can be made visible in brightfield microscopy by defocusing the microscope (14). Defocusing translates phase differences into intensity differences in microscopic imaging (15). However, phase information deteriorates with decreasing spatial coherence of the light source (16). The combination of pinhole and monochromatic filter produces a quasi-coherent wave front, thereby strongly improving phase contrast in defocused images. Our results show that pinhole illumination combined with defocused image acquisition results

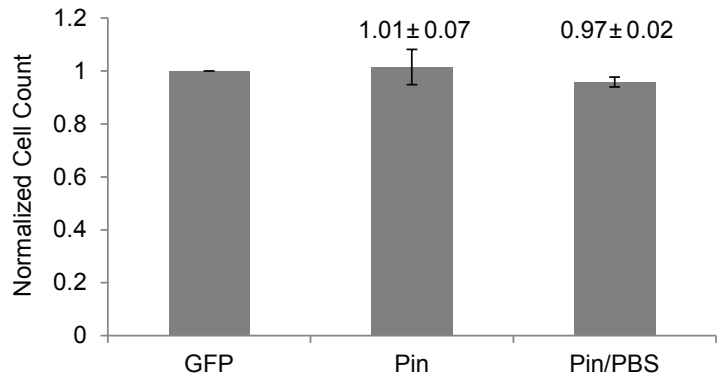

Figure 4. Counting of dense confluent cell layers. SHEP-GFP cells were seeded at very high cell densities of ~5 million per well and allowed to grow for 1 day, resulting in a fully confluent cell layer. Cells were imaged with fluorescence (GFP), pinhole (Pin), and pinhole + PBS (Pin/PBS) techniques. Cell counts of pinhole illuminated images with and without PBS incubation were normalized against fluorescence images of the same viewing field (mean ± SD, n = 6).

in bright-field images with high contrast. This can be conceptualized as each cell body acting as a miniature lens to produce a bright, central spot below the cell layer. Such spots can easily be identified through threshold analysis and used for cell counting.

Adding a narrow-spectrum color filter to the light path improves coherence and contrast in our images. This could be seen as preventing chromatic dispersion from the cell-body lenses. Although a green filter was used initially to enhance contrast with the pink cell culture medium, experiments with a red monochromatic filter (Kodak Wratten filter #61) yielded equally good results (not shown).

Swelling cell bodies by treating with PBS enhanced cell curvature and thus enhanced the lensing effect, substantially improving cell counting accuracy. Under our experimental conditions, short-term incubation in PBS had no measurable effect on growth parameters, permitting two or more independent counts over the course of an experiment. While counting accuracy was improved at high cell densities, the technique reached its limit when imaging cells had grown into multiple layers.

Previously published strategies to enhance image contrast for bright-field microscopy have used contrast differentials from multiple z-stacked images (9,10), or have determined cell density through measuring the size of confluent areas and multiplying by a calculated density factor (17). These strategies are best suited for automated image acquisition. The method presented here permits cell counting by use of a simple bright-field microscope with very minor hardware modifications. It allows repeated, quick, and simple counting in routine cell culture environments and should be a versatile quality-control tool for a variety of mammalian cell culture applications.

Acknowledgments

The SH-EP cell line was a gift from R. König, F Westermann and M. Schwab (DKFZ, Heidelberg, Germany). We gratefully acknowledge the use of the fluorescence microscope of S. Sakiyama-Elbert, BME Washington University in St. Louis. LLD wishes to thank G.F. Schreiner, Washington University Medical School, for giving access to his laboratory and equipment while the imaging method was refined. This research was in part financially supported by the DRC at Washington University (NIH Grant No. 5 P30 DK020579), the German Science Foundation (DFG, BI 1409/1-1), and by the German Ministry for Science and Education (BMBF, NGFN-Plus 01GS08132, GERAMY 01GM1107C). This paper is subject to the NIH Public Access Policy.

Competing interests

The authors declare no competing interests.

References

1. **Ricardo, R. and K. Phelan.** 2008. Counting and determining the viability of cultured cells. J Vis Exp.
2. **Park, C.H., B.F. Kimler, and T.K. Smith.** 1985. Comparison of the supravital DNA dyes Hoechst 33342 and DAPI for flow cytometry and clonogenicity studies of human leukemic marrow cells. Exp. Hematol. *13*:1039-1043.
3. **Batra, R., N. Harder, S. Gogolin, N. Diessl, Z. Soons, C. Jager-Schmidt, C. Lawerenz, R. Eils, et al.** 2012. Time-lapse imaging of neuroblastoma cells to determine cell fate upon gene knockdown. PLoS ONE *7*:e50988.
4. **Curl, C.L., C.J. Bellair, T. Harris, B.E. Allman, P.J. Harris, A.G. Stewart, A. Roberts, K.A. Nugent, and L.M. Delbridge.** 2005. Refractive index measurement in viable cells using quantitative phase-amplitude microscopy and confocal microscopy. Cytometry A *65*:88-92.
5. **Ali, R., M. Gooding, T. Szilágyi, M. Christlieb, and M. Brady.** 2011. Automatic segmentation of adherent biological cell boundaries and nuclei from brightfield microscopy images. Machine Vision and Applications:online publication.
6. **Tscherepanow, M., N. Jensen, and F. Kummert.** 2008. An incremental approach to automated protein localisation. BMC Bioinformatics *9*:445.
7. **Kvarnström, M., K. Logg, A. Diez, K. Bodvard, and M. Kall.** 2008. Image analysis algorithms for cell contour recognition in budding yeast. Opt. Express *16*:12943-12957.
8. **Mölder, A., M. Sebesta, M. Gustafsson, L. Gisselson, A.G. Wingren, and K. Alm.** 2008. Non-invasive, label-free cell counting and quantitative analysis of adherent cells using digital holography. J. Microsc. *232*:240-247.
9. **Selinummi, J., P. Ruusuvuori, I. Podolsky, A. Ozinsky, E. Gold, O. Yli-Harja, A. Aderem, and I. Shmulevich.** 2009. Bright field microscopy as an alternative to whole cell fluorescence in automated analysis of macrophage images. PLoS ONE *4*:e7497.
10. **Dehlinger, D., L. Suer, M. Elsheikh, J. Pena, and P. Naraghi-Arani.** 2013. Dye free automated cell counting and analysis. Biotechnol. Bioeng. *110*:838-847.
11. **Byun, J., M.R. Verardo, B. Sumengen, G.P. Lewis, B.S. Manjunath, and S.K. Fisher.** 2006. Automated tool for the detection of cell nuclei in digital microscopic images: application to retinal images. Mol. Vis. *12*:949-960.
12. **Selinummi, J., J. Seppala, O. Yli-Harja, and J.A. Puhakka.** 2005. Software for quantification of labeled bacteria from digital microscope images by automated image analysis. Biotechniques *39*:859-863.
13. **Zernicke, F.** 1935. Das Phasenkontrastverfahren bei der mikroskopischen Beobachtung. Zeitschrift für Technische Physik *16*:454-457.
14. **Agero, U., C.H. Monken, C. Ropert, R.T. Gazzinelli, and O.N. Mesquita.** 2003. Cell surface fluctuations studied with defocusing microscopy. Phys. Rev. E Stat. Nonlin. Soft Matter Phys. *67*:051904.
15. **Teague, M.R.** 1983. Deterministic phase retrieval: a Green's function solution. J. Opt. Soc. Am. *73*:1434-1441.
16. **Waller, L.** Phase imaging with partially coherent light. in SPIE BiOS. 2013. International Society for Optics and Photonics.
17. **Topman, G., O. Sharabani-Yosef, and A. Gefen.** 2011. A method for quick, low-cost automated confluency measurements. Microsc. Microanal. *17*:915-922.

Received 03 April 2013; accepted 12 June 2013.

Address correspondence to Jan Bieschke, Washington University in St. Louis, Department of Biomedical Engineering, St. Louis, MO. E-mail: bieschke@wustl.edu

To purchase reprints of this article, contact: biotechniques@fosterprinting.com